BMC Pediatrics

RESEARCH

Open Access

Evaluation of postoperative renal function in infants with congenital hydronephrosis using ROI from ultrasound technique in renography

Siyu Ren[1], Airui Wu[1], Xiaoxia Wen[1] and Deshan Zhao[1*]

Abstract

The aim of this study was to assess the efficacy of GFR measured using ROI from ultrasound technique in diuretic renography for evaluating postoperative outcomes in infants under one year old with congenital hydronephrosis. A retrospective analysis was conducted on thirty infants who underwent abdominal ultrasound and diuretic renography before and after surgery, obtaining preoperative and postoperative gGFRs and uGFRs (measured using ROI from ultrasound technique) determined using the Gates method and ultrasonic-assisted drawing ROI technique, respectively. A comparative study was performed on total GFR as well as individual kidney GFR before and after intervention. The preoperative and postoperative total and single uGFRs were significantly lower than gGFRs, while the postoperative total and single renal function, along with relative renal function in the hydronephrotic kidneys, were also significantly higher than the preoperative results ($p < 0.05$). Among 30 infants, 23 cases exhibited substantial recovery of renal function in their hydronephrotic kidneys after surgery, 2 cases did not show significant improvement, while 5 cases continued to experience deterioration in renal function. The GFR measured using ROI from ultrasound technique provides a more accurate assessment of renal function changes before and after surgery in infants under one year old with congenital hydronephrosis, facilitating an effective evaluation of postoperative treatment efficacy.

Keywords Congenital hydronephrosis, Renal function, Diuretic renography, Ultrasound, Region of interest

Introduction

The developmentally anomalous urinary system primarily accounts for congenital hydronephrosis among infants; notably, stenosis at the ureteropelvic junction stands out as its most prevalent etiology [1]. The prolonged presence of hydronephrosis, caused by severe urinary tract obstruction, is a significant factor contributing to impaired kidney function. This condition ranks high among the causes leading to impaired kidney functions. Prenatal ultrasound screening allows for the diagnosis of prenatal hydronephrosis, with incidence rates ranging from 0.5% to 1% across all pregnancies [2, 3]. As a key tool for prognostic monitoring purposes related to the severity of this condition postnatally, ultrasound not only tracks changes but also offers insights into structural alterations while indirectly indicating functional impairments based on variations observed within kidney volumes. Direct assessment methods, such as radioactive diuretic renography, enable monitoring changes specific to affected kidneys' functions and aid in determinations regarding progression or amelioration associated with congenital hydronephrosis [4]. However, limitations presented by factors like patient age, height, and weight,

*Correspondence:
Deshan Zhao
deshanzh@163.com
[1] Department of Nuclear Medicine, The Second Hospital of Shanxi Medical University, No. 382 Wuyi Road, Taiyuan, Shanxi Province 030001, China

water load before renography, renal region of interest (ROI), renal depth, and so on, can influence the measurement glomerular filtration rate (GFR) values of the Gates method and impact its clinical applicability [5]. In particular, drawing ROIs for patients suffering from moderate-to-severe forms could potentially introduce inaccuracies due to susceptibility towards radioactive scattering within these conditions. This results in errors that ultimately affect GFR accuracy. To address these challenges, a proposed solution involves employing an ultrasonic-assisted drawing ROI technique when delineating renal ROIs during renography procedures involving infants with hydronephrosis. This approach aims at mitigating potential inaccuracies arising from erroneous ROI outlines affecting GFR measurements. Furthermore, a comparative analysis between preoperative and postoperative gGFR and uGFR measured by both Gates method and ultrasonic-assisted drawing ROI technique respectively will be conducted. The ultimate goal lies in establishing a reliable imaging methodology capable of accurately evaluating the kidney functions of infants, hence enabling well-informed therapeutic decisions. Static renal imaging is a radioactive examination method used to assess the position, size, shape, and functions of the kidneys. Typically, static renal imaging reveals that the kidney has a broad bean shape with well-defined edges and a clear outline. The use of static renal imaging can more accurately delineate the kidney ROI, and the comparison of GFR obtained from this ROI with uGFR can provide a preliminary understanding of the reliability of uGFR.

Materials and methods

General material

A retrospective analysis was performed on a cohort of thirty infants diagnosed with congenital hydronephrosis—comprising twenty-four males and six females—who underwent both pre- and post-operative abdominal ultrasonography at Shanxi Children's Hospital between January 2018 and December 2023; additionally, they received diuretic renography using technetium-99 m-labeled DTPA at The Second Hospital of Shanxi Medical University during this period. The pre-operative ages ranged from thirty-three days to twelve months, while the post-operative assessments were conducted within six to ten months following surgery. Key demographic data for all patients included age (pre-op:3.16 ± 2.63 months; post-op:12.26 ± 5.31 months), height (pre-op:61.15 cm ± 8.04 cm; post-op:74.65 cm ± 14.99 cm), and weight (pre-op:6.58 kg ± 2.44 kg; post-op:10.23 kg ± 2.05 kg). Among these patients, bilateral hydronephrosis was observed in three cases, distinguished by severe involvement on one side and mild involvement on the contralateral side; unilateral severe hydronephrosis was identified in twenty-seven cases. The severity of hydronephrosis across all patients can be attributed to stricture occurring at the ureteropelvic junction on the affected side. Routine prenatal and postnatal ultrasound monitoring is undertaken at Shanxi Children's Hospital. Progressive aggravation of hydronephrosis on the severely affected side prompted surgical intervention by urologists. Interventions included stent placement at sites of the stenotic ureteropelvic junctions in affected kidneys (twenty-four cases), pyeloureterostomy (three cases), and a local diversion implemented at hydronephrotic sites (three cases). Raw data for diuretic renography preoperatively and postoperatively along with renal ultrasonographic morphological indexes within the same week were collected. Subsequently, rework in gall of the raw data gathered from the diuretic renography studies was carried out. Two approaches were pursued according to relevant guidelines and regulations.

Radiotracer and imaging equipment

Ultrasonography was conducted using a Volusion E8 Expert scanner manufactured by General Electric Company, USA. Diuretic renography was performed using a dual-head gamma camera (SPECT, Discovery NM/CT 670, General Electric Company, USA) equipped with a low-energy high-resolution collimator and set at a 20% energy window with a photopeak of 140 keV. The labeling efficiency of ^{99m}Tc-DTPA exceeded 95%. Pentetate (DTPA) was provided by Beijing Xinkesida Medical Technology Co. Ltd., Beijing, China. Tc-99 m was supplied by Atom High-Tech Co. Ltd., Beijing, China.

Diuretic renography

All infants were fed on water or breast milk at a standardized rate of 5 ml/kg for adequate hydration over a period of 30 to 60 min prior to the study, in turn administered chloral hydrate with a concentration of 10% through rectum for the purpose of sedation [6]. The patient's height and weight were recorded. The patients were in a supine position during the procedure, and administered ^{99m}Tc-DTPA intravenously at a dosage of 3.7 MBq/kg (with a minimum total dose of 37 MBq). The preoperative dose was 41.16 ± 6.87 MBq (range: 38.11 ~ 48.47 MBq), while the postoperative dose ranged from 46.62 to 85.47 MBq with a mean of 59.94 ± 12.29 MBq. Following intravenous bolus injection of ^{99m}Tc-DTPA, image data would be acquisited in posterior view using a matrix size of 64 × 64 and a zoom of 1.0 at frame rates of 30 frames/2 s and 180 frames/10 s. Furosemide was administered at a standard dose of 1 mg/kg within a time frame of 15 min [7], with a volume ranging from 0.3 to 0.5 ml.

Static renal imaging

^{99m}Tc-DMSA static renal imaging was performed within 1 ~ 3 days after diuretic renography. ^{99m}Tc-DMSA was administered intravenously with a dose of 3.7 MBq/kg (average dose: 58.63 ± 9.29 MBq, dose range: 45.51~69.46 MBq) and a volume of 0.3 ~ 0.5 ml. The patient was examined in the supine position. The renal images were acquired at posterior, anterior views (700 kilocounts/view), left and right lateral views (300 kilocounts/view) in a 128 × 128 matrix format at 1 ~ 2 h after the injection of ^{99m}Tc-DMSA.

Processing of kidney image data and determination of GFR

Delineation of ROI

The computer software utilized possessed a measurement distance function with units expressed in millimeters (mm). In the processing of kidney image data utilizing the Gates method, the grayscale levels of all patient images were standardized to a relatively fixed range on the GE medical display for SPECT/CT. The delineation of ROI for the kidneys involved drawing ROIs along the peripheral edges of both kidney images in renography, while excluding any fluid accumulation within the pelvis, allowing for precise measurements of both the maximum length (from the upper pole to the lower pole of the kidney) and width (from the hilum to the outer margin of the kidney) of the kidneys by assessing distances between their superior and inferior margins as well as their medial (hilum) and lateral borders. A closed circular ROI was formed within the kidney, which served as a reference for further analysis

Determination of GFR

Image data obtained from dynamic renography underwent processing using the Xeleris image processing system. After ROIs of two kidneys were delineated, inputting infant's height and weight to Gates algorithm following the procedural guidelines, single kidney GFR as well as GFR for both kidneys were automatically calculated.

Gates' formula[8]: [8] $GFR(mL/min) = 9.81272 \times \%RU - 6.82519$

$$\%RU = \frac{Cr/e^{-0.153R} + Cl/e^{-0.153L}}{Cpre - Cpost}$$

%RU = % uptake / total injected dose at 2 ~ 3 min post injection.

Cr = counts in the right kidney for 1 min at 2 ~ 3 min post injection.

Cl = counts in the left kidney for 1 min at 2 ~ 3 min post injection.

Cpre = pre-injection counts / min.

Cpost = post-injection counts / min.

In Gates' method (renal depth was estimated by Tønnesen formula).

R = right renal depth (cm) = 13.3 × W/H + 0.7

L = left renal depth (cm) = 13.2 × W/H + 0.7

W/H = body weight (kg) / height (cm).

GFR measured using ROI from ultrasound-assisted drawing ROI technique

The maximum length and width of the kidney on the coronal plane were measured using ultrasonography. The maximum length was defined as the distance from the upper pole to the lower pole of the kidney, while the maximum width was measured from the hilum to the outer margin of the kidney on the coronal plane. These measurements obtained through ultrasonography were then used to determine corresponding length and width of the kidneys on original renography image. Therefore, by applying formulas such as: (kidney length in renography-kidney length in ultrasound)/2 and (kidney width in renography-kidney width in ultrasound)/2, the upper and lower margins as well as the medial and lateral margins of the kidney ROI in renography are adjusted by subtracting half of the respective differences in kidney length and width between renography and ultrasound. Then during processing the original kidney image data using the Gates method for GFR determination, the renal ROI was reconstructed utilizing four endpoints adjusted on a composite image taken between 2 ~ 3 min in renography, followed by computation of uGFR value. Reprocessing and interpretation of images were collaboratively performed by two proficient nuclear medicine physicians who reached a consensus to ensure consistent outcomes.

Statistical analysis

All statistical analysis was done with SPSS Statistics version 25.0. Quantitative data were presented as mean ± standard deviation and analyzed using paired t-test. A p-value of less than 0.05 was considered statistically significant.

Results

Comparison of gGFR determined using the Gates method and uGFR measured using ROI from ultrasound technique in infants with hydronephrosis before and after surgery

The preoperative and postoperative total uGFR and single uGFR of the infants showed a significant decrease compared to gGFR, with statistically significant differences observed between the groups ($p < 0.01$). The uGFR of total kidneys and individual kidney in infants demonstrates closer proximity to actual GFR values compared to the gGFR [9, 10]. Furthermore, the

postoperative renal function of both total kidneys and individual kidney, as well as the relative renal function of hydronephrotic kidneys, exhibited a significant increase compared to the preoperative results ($p < 0.05$) (Table 1, Fig. 1). In Fig. 1, Fig a and Fig b illustrate that among 19 left kidneys with hydronephrosis, 7 had

Table 1 Comparison of uGFR and gGFR of total kidneys and individual kidney before and after surgery (x ± s, ml·min^{-1}·1.73m^2)

		Preoperation			Postoperation		
	Number(n)	gGFR	uGFR	t(p)	gGFR	uGFR	t(p)
TKids	30	80.20 ± 18.46[a,d]	66.01 ± 17.71[a]	[a]–4.7 (0.01) [d]8.79(0.01)	101.73 ± 21.70[a,d]	81.83 ± 17.45[a]	[a]–4.4 (0.01) [d]8.90(0.01)
LKid	30	38.26 ± 15.60b[e]	31.85 ± 14.98[b]	b–3.7 (0.01) [e]5.04(0.01)	50.24 ± 19.08[b,e]	42.02 ± 14.32[b]	[b]4.1 (0.01) [e]5.38(0.01)
RKid	30	41.98 ± 13.50[c,f]	33.28 ± 11.21[c]	[b]–4.6 (0.01) [f]–7.33(0.01)	51.19 ± 17.20[c,f]	40.72 ± 13.10[c]	[c]–4.8 (0.01) [f]8.14(0.01)

gGFR GFR measured by Gates method, *uGFR* GFR measured using ROI from ultrasound technique, *TKids* total kidneys, *LKid* left kidney, *RKid* right kidney, $p < 0.05$ had statistically difference

[a] Comparation between preoperative gGFR and postoperative gGFR (t = −4.7, $p < 0.01$) or between preoperative uGFR and postoperative uGFR (t = −4.4, $p < 0.01$) in TKids

[b] Comparation between preoperative gGFR and postoperative gGFR (t = −3.7, $p < 0.01$) or between preoperative uGFR and postoperative uGFR (t = 4.1, $p < 0.01$) in LKid

[c] Comparation between preoperative gGFR and postoperative gGFR (t = −4.6, $p < 0.01$) or between preoperative uGFR and postoperative uGFR (t = −4.8, $p < 0.01$) in RKid

[d] Comparation between preoperative gGFR and uGFR (t = 8.79, $p < 0.01$) or between postoperative gGFR and uGFR (t = 8.90, $p < 0.01$) in TKids

[e] Comparation between preoperative gGFR and uGFR (t = 5.04, $p < 0.01$) or between postoperative gGFR and uGFR (t = 5.38, $p < 0.01$) in LKid

[f] Comparation between preoperative gGFR and uGFR (t = −7.33, $p < 0$ 0.01) or between postoperative gGFR and uGFR (t = 8.14, $p < 0.01$) in RKid

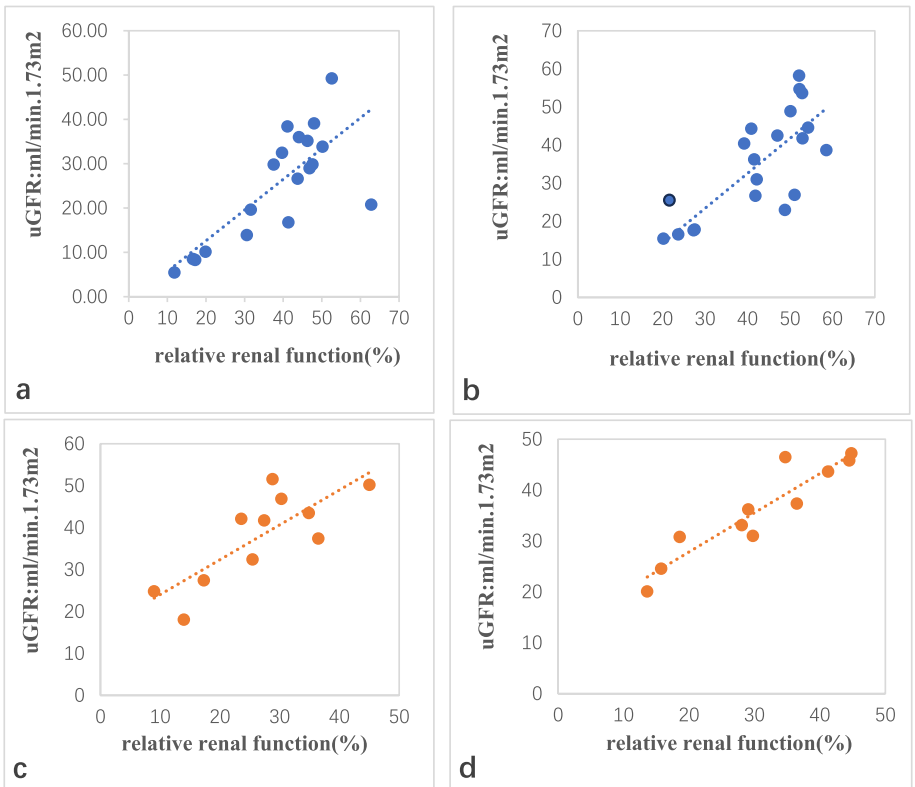

Fig. 1 uGFR: GFR measured using ROI from ultrasound technique, RRF:relative renal function. **a** The relation between preoperative uGFR and its RRF in 19 infants with hydronephrotic left kidney; **b** The relation between postoperative uGFR and its RRF in 19 infants with hydronephrotic left kidney; **c** The relation between preoperative uGFR and its RRF in 11 infants with hydronephrotic right kidney; **d** The relation between postoperative uGFR and its RRF in 11 infants with hydronephrotic right kidney

lower GFR and relative renal function preoperatively, with mildly decreased and normal GFR and relative renal function in 12 kidneys; postoperatively, GFR and relative renal function improved significantly in 16 kidneys, with a decrease in 3 kidneys. Fig c and Fig d illustrate that among 11 right kidneys with hydronephrosis, 3 had lower GFR and relative renal function preoperatively, with mildly decreased and normal GFR and relative renal function in 8 kidneys; postoperatively, GFR and relative renal function improved significantly in 9 kidneys, with a decrease in 2 kidneys.

Comparison of gGFR and uGFR in infants with hydronephrotic kidneys before and after surgery

The comparison of gGFR and uGFR of normal and hydronephrotic kidneys in infants before and after surgery, revealed a significant increase in both gGFR and uGFR postoperatively compared to the preoperative period ($p < 0.01$) (Table 2). Among 30 infants, significant recovery of renal function in the hydronephrotic kidney was observed in 23 cases after surgery, while 2 cases did not exhibit substantial improvement and 5 cases continued to experience functional deterioration (Fig. 2). In Fig. 2,

Table 2 Comparison of gGFR and uGFR of normal and hydronephrotic kidneys before and after surgery ($x \pm s$, $ml \cdot min^{-1} \cdot 1.73m^2$)

		Preoperation			Postoperation		
	Numb(n)	gGFR	uGFR	t(p)	gGFR	uGFR	t(p)
Kidhn	30	33.30 ± 13.70	26.83 ± 11.30	−4.16(0.01)	40.66 ± 18.31	33.15 ± 14.32	3.35(0.01)
Kidnorm	30	48.50 ± 11.74	39.30 ± 11.11	−7.61(0.01)	60.41 ± 12.78	48.90 ± 9.73	9.67(0.01)

gGFR GFR measured by Gates method, *uGFR* GFR measured by ultrasonic-assisted technique, *LKidhn* kidney with hydronephrosis, *Kidnorm* normal kidney. $p < 0.05$ had statistical difference

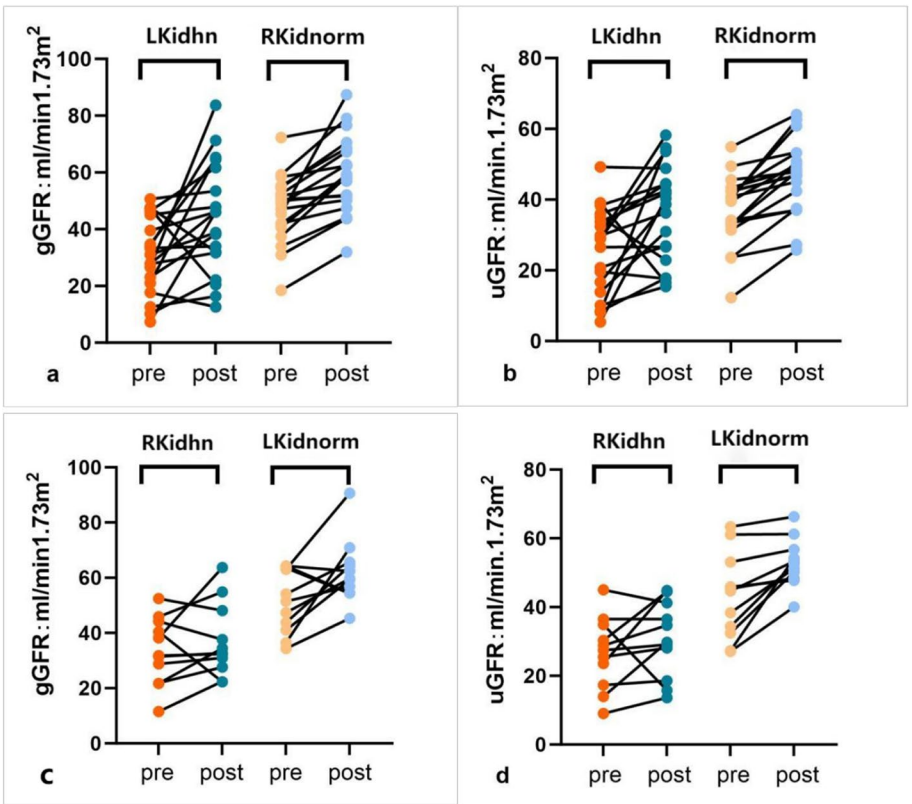

Fig. 2 gGFR:GFR measured by Gates method, uGFR:GFR measured using ROI from ultrasound technique. pre:preoperation, post:postoperation. LKidhn:left kidney with hydronephrosis, RKidnorm:normal right kidney, RKidhn:right kidney with hydronephrosis, LKidnorm:normal left kidney. **a** Comparison of gGFRs between pre- and postoperation in infants with LKidhn and RKidnorm; **b** Comparison of uGFRs between pre- and postoperation in infants with LKidhn and RKidnorm; **c** Comparison of gGFRs between pre- and postoperation in infants with RKidhn and LKidnorm; **d** Comparison of uGFR between pre- and postoperation in infants with RKidhn and LKidnorm

Fig a and Fig b illustrate that among 19 left kidneys with hydronephrosis, their gGFR and uGFR were low before surgery, and both gGFR and uGFR increased significantly in 15 kidneys after surgery, with no significant change in 1 kidney and a slight decrease in 3 kidneys. In 19 normal right kidneys, both gGFR and uGFR increased after surgery. Fig c and Fig d illustrate that among 11 right kidneys with hydronephrosis, thire gGFR and uGFR were low before surgery, and both gGFR and uGFR increased significantly in 9 kidneys after surgery, with no significant change in 1 kidney and a slight decrease in 2 kidneys. In 11 normal left kidneys, gGFR increased in 9 kidneys after surgery, while 2 kidneys had a slight decrease in gGFR, and uGFR increased in all kidneys. Two kidneys with a slight decrease in gGFR were considered to be affected by errors caused by scattering when drawing the ROI of the kidney.

Comparison of sGFR and uGFR in infants with hydronephrosis before surgery.

A comparison between sGFR measured by static renal imaging and uGFR measured using ROI from ultrasound technique in 20 infants with moderate to severe hydronephrosis prior to surgery revealed no significant difference($p > 0.05$) (Table 3).

Discussion

Urinary tract dilation (UTD), including its most prevalent form, hydronephrosis (HN), is a commonly observed condition during pregnancy. The prevalence of prenatal hydronephrosis is approximately twofold higher in males compared to females [11]. Spontaneous resolution of HN occurs in about 75%~80% of children within a few years following birth, while a small number exhibit progressive deterioration necessitating surgical intervention to alleviate urinary obstruction [12]. Congenital anomalies, particularly ureteropelvic stenosis, are primary etiologies of hydronephrosis and significant contributors to chronic renal failure development in children [13]. Early differential diagnosis and timely therapeutic intervention play pivotal roles in mitigating the progression of renal function impairment. Abdominal ultrasound monitors hydronephrosis progression by evaluating changes in pelvicalyceal dilation and quantifying morphological parameters related to the kidneys such as renal cortical length, width, and thickness to infer alterations in renal function [4, 14]. Diuretic renography assesses changes in renal function due to hydronephrosis offering superior advantages for enhancing individual renal function assessment [15, 16]. Due to the severe degree of hydronephrosis in infants with moderate and severe hydronephrosis, caused by significant urinary tract obstruction, the renal cortex is visibly compressed and atrophied. The impairment of renal function is relatively serious, with a large amount of radioactive scattering in the hydronephrotic area. This, combined with surrounding background interference and limitations in resolution of the radioactive imaging equipment, makes it difficult to distinguish the kidney contour, resulting in significant errors.

During diuretic renography, the kidney contour image on the side affected by hydronephrosis is unclear, leading to potential large errors in delineating the kidney ROI. Particularly after surgical intervention when hydronephrosis subsides, there can be substantial differences in the kidney ROI delineated compared to pre-surgery measurements. This can impact accurate evaluation of surgical efficacy to some extent. However, ultrasound measurements of long and short diameters on the side affected by hydronephrosis are more realistic and accurate. If these results are input into an image processing program for diuretic renography to assist in mapping ROI for infants and young children affected by hydronephrosis, theoretically a more precise GFR can be obtained. This may hold greater value for evaluating renal function before and after surgical treatment. The utilization of ultrasound is aimed at bringing the ROI closer to reality in order to obtain a more accurate GFR value. Although ultrasound measurements may have some subjectivity, conducting measurements by the same sonographer minimizes inter-child measurement errors. Additionally, ultrasound equipment offers superior resolution compared to renography. Out of 30 infants, we randomly selected 20 for static renal imaging before surgery and found that the GFR of the infants calibrated by static renal imaging was closer to the uGFR value, indicating a potential overestimation of gGFR. In line with this principle, we utilized ultrasound-derived measurements of renal length and width in infant patients to define ROIs encompassing the kidneys. We conducted a comparative study on the renal function of 30 infants under one year old with hydronephrosis before and after surgery. During infancy and early childhood, renal development is not yet fully mature, resulting in a relatively smaller number of available functional nephrons compared to older children. Consequently, GFR in a single kidney is

Table 3 Comparison of sGFR and uGFR in infants with hydronephrosis before surgery ($x \pm s$, $ml \cdot min^{-1} \cdot 1.73m^2$)

	Number (n)	sGFR	uGFR	t(p)
Kidnorm	20	62.05 ± 13.75	61.53 ± 14.07	-1.19(0.25)
Kidhn	20	35.30 ± 11.32	36.01 ± 11.23	-1.59(0.13)

sGFR GFR measured by ^{99m}Tc-DMSA static renal imaging, *uGFR* GFR measured using ROI from ultrasound technique. *Kidnorm* normal kidney, *Kidhn* kidney with hydronephrosis. $p < 0.01$ had statistically difference

also comparatively lower. The research findings suggest that there is a concomitant decline in renal GFR with decreasing age [9, 10]. Our research indicated that uGFR measured using ROI from ultrasound technique tends to exhibit slightly lower values compared to gGFR based on the Gates method. Additionally, our findings align closely with those from previous studies [9, 10], thereby providing a more accurate estimation of GFR during infancy and early childhood. The disparity in GFRs measured by the two methodologies may be attributed to the relatively diminished size of pediatric kidneys during infancy and early childhood as well as slightly larger renal ROIs determined by the Gates method. In this study, the infants were relatively young at preoperative assessment, followed up 6 ~ 10 months after surgery. Following surgery, there was significant improvement in total renal function observed in all patients relative to their preoperative status due to rapid overall organ and tissue development occurring during this critical period for infants. After comparing preoperative and postoperative renal function among 30 infants who underwent relief from urinary obstruction, it was observed that there was a clear improvement of relative renal function in 23 cases, whereas no significant improvement was observed in two cases. Furthermore, five cases showed continued worsening of renal injury following surgical intervention. This situation may be attributed to a delayed timing of surgical intervention or sustained inflammatory response within the kidney elicited by urinary obstruction. When the degree of renal damage on the side with hydronephrosis reaches a certain threshold or when there is sustained inflammatory response within the kidney, it initiates a positive feedback loop in the impairment process. Even if detrimental factors are promptly terminated at this moment, the short-term progression of damage may remain inevitable.

The results of animal experimental studies indicated that localized congestion of connective tissue and infiltration of white blood cells occur at the site of stenosis in the ureteropelvic junction, leading to an irreversible local inflammatory response and fibrosis, accompanied by impaired peristaltic function of the ureter [17]. Concurrently, it triggers excessive production of reactive oxygen species (ROS) within the ipsilateral kidney, thereby initiating modifications in apoptotic pathways that facilitate inflammation, oxidative stress, and fibrosis progression. Consequently, this results in renal parenchymal damage and subsequent functional deterioration in the kidney [18]. Furthermore, urinary obstruction-induced systemic immune response regulation may potentially impact contralateral ureter and kidney functionality [17]. Additionally, postoperative gGFR significantly decreased in one patient and mildly decreased in another in the normal right kidney assessed by the Gates method. However, uGFR measured using ROI from ultrasound technique was found to be comparable to or slightly increased compared to preoperative values in both patients. The observed discrepancy may be attributed to precision issues when delineating ROI in kidneys or prolonged obstruction of contralateral kidney with hydronephrosis triggering a systemic immune response subsequently impacting corresponding kidney functionality on that side [17]. This finding implies that ultrasound-assisted drawing ROI technique for measuring uGFR may offer enhanced accuracy potential. The study's findings suggest that applying ROI from ultrasound techniques for delineating renal ROI during renography offers significant advantages for assessing renal function and evaluating postoperative efficacy in infants with hydronephrosis. Currently, this method is limited to assessing the hydronephrotic renal function in infants only, further validation is required before extending its application to children and adults. It is important to note that this study has a limited sample size and short follow-up period which could introduce some degree of bias into the results; hence we plan to progressively increase sample size and extend follow-up duration.

Acknowledgements
Not applicable.

Clinical trial number
(2022) YX No.(122).

Authors' contributions
Ds Z: Conceptualization, Investigation, Methodology, Project Administration, Resources, Supervision, Validation, Formal Analysis, Software, Funding Acquisition; Sy R: Conceptualization, Investigation, Methodology, Writing-Original Draft, Date Curation, Software; Formal Analysis, Validation; Ar W: Investigation, Writing-Original Draft, Date Curation, Software; Formal Analysis, Validation; Xx W: Investigation, Writing-Original Draft, Date Curation, Software; Formal Analysis, Validation

Funding
Not applicable.

Data availability
No datasets were generated or analysed during the current study.

Declarations

Ethics approval and consent to participate
We confirm that written informed consent was obtained from the guardians of all participants. The study was conducted in accordance with the Declaration of Helsinki, and the protocol was approved by the Ethics Committee of the Second Hospital of Shanxi Medical University under petition number (2022) YX No.(122).

Consent for publication
We confirm that the consent for publication was obtained from the guardians of all participants. We confirm that the "written informed consent" was given from the guardians of all patients for their children personal or clinical details along with any identifying images to be published in this study.

Competing interests
The authors declare no competing interests.

Received: 5 September 2024 Accepted: 11 November 2024
Published online: 21 November 2024

References

1. Cai PY, Lee RS. Ureteropelvic Junction Obstruction/Hydronephrosis. Urol Clin North Am. 2023. https://doi.org/10.1016/j.ucl.2023.04.001.
2. Woodward M, Frank D. Postnatal management of antenatal hydronephrosis. BJU Int. 2002. https://doi.org/10.1046/j.1464-4096.2001.
3. Yalçınkaya F, Özçakar ZB. Management of antenatal hydronephrosis. Pediatr Nephrol. 2020. https://doi.org/10.1007/s00467-019-04420-6.
4. Guo K, Zhao D. The correlation between GFR and unit renal volume in infants with hydronephrosis measured by two imaging methods. Sci Rep. 2023. https://doi.org/10.1038/s41598-023-46996-y.
5. Pang X, Li F, Huang S, Wang C, Zhang T, Hu Z, et al. A Novel Method for Accurate Quantification of Split Glomerular Filtration Rate Using Combination of Tc-99m-DTPA Renal Dynamic Imaging and Its Plasma Clearance. Dis Markers. 2021. https://doi.org/10.1155/2021/6643586.
6. Gernhold C, Kundtner N, Steinmair M, Henkel M, Oswald J, Haid B. Sedation Rate Reduction in Paediatric Renal Nuclear Medicine Examinations: Consequences of a Targeted Audit. Children (Basel). 2021;. https://doi.org/10.3390/children8050424.
7. Kazlauskas V, Cekuolis A, Bilius V, Anglickis M, Verkauskas G. Diuretic Enhanced Ultrasonography in the Diagnosis of Pyeloureteral Obstruction. Medicina (Kaunas).2019. https://doi.org/10.3390/medicina55100670.
8. Gates GF. Split Renal Function Testing Using Tc–99m DTPA: A Rapid Technique for Determining Differential Glomerular Filtration. Clin Nucl Med. 1983;8:400–7.
9. Piepsz A, Tondeur M, Ham H. Revisiting normal (51)Cr-ethylenediaminetetraacetic acid clearance values in children. Eur J Nucl Med Mol Imaging. 2006. https://doi.org/10.1007/s00259-006-0179-2.
10. Schwartz GJ, Work DF. Measurement and estimation of GFR in children and adolescents. Clin J Am Soc Nephrol. 2009. https://doi.org/10.2215/CJN.01640309.
11. Expert Panel on Pediatric Imaging; Brown BP, et al. ACR Appropriateness Criteria® Antenatal Hydronephrosis-Infant. J Am Coll Radiol. 2020;17. https://doi.org/10.1016/j.jacr.2020.09.017.
12. Rickard M, Dos Santos J, Keunen J, Lorenzo AJ. Prenatal hydronephrosis: Bridging pre- and postnatal management. Prenat Diagn. 2022. https://doi.org/10.1002/pd.6114.
13. Deng QF, Chu H, Peng B, Liu X, Cao YS. Outcome analysis of early surgery and conservative treatment in neonates and infants with severe hydronephrosis. J Int Med Res. 2021;49:3000605211057866. https://doi.org/10.1177/03000605211057866.
14. Zhang H, Zhang L, Guo N. Validation of "urinary tract dilation" classification system: Correlation between fetal hydronephrosis and postnatal urological abnormalities. Medicine (Baltimore). 2020. https://doi.org/10.1097/MD.0000000000018707.
15. Dias CS, et al. Exames de imagem na avaliação de anomalias urológicas em lactentes com hidronefrose fetal: avanços e controvérsias [Imaging for evaluation of urologic abnormalities in infants with fetal hydronephrosis: advances and controversies]. J Bras Nefrol. 2012. https://doi.org/10.5935/0101-2800.20120031.
16. Taylor AT, et al. SNMMI Procedure Standard/EANM Practice Guideline for Diuretic Renal Scintigraphy in Adults With Suspected Upper Urinary Tract Obstruction 1.0. Semin Nucl Med. 2018. https://doi.org/10.1053/j.semnuclmed.2018.02.010.
17. Reicherz A, et al. Ureteral Obstruction Promotes Ureteral Inflammation and Fibrosis. Eur Urol Focus. 2023. https://doi.org/10.1016/j.euf.2022.09.014.
18. Aranda-Rivera AK, Cruz-Gregorio A, Aparicio-Trejo OE, Ortega-Lozano AJ, Pedraza-Chaverri J. Redox signaling pathways in unilateral ureteral obstruction (UUO)-induced renal fibrosis. Free Radic Biol Med. 2021. https://doi.org/10.1016/j.freeradbiomed.2021.05.034.

Publisher's Note